

RESEARCH

Open Access



Alternative boronic acids in the detection of Mycolactone A/B using the thin layer chromatography (f-TLC) method for diagnosis of Buruli ulcer

Gideon A. Akolgo¹, Benjamin M. Partridge², Timothy D. Craggs² and Richard K. Amewu^{1*}

Abstract

Background *Mycobacterium ulcerans* is the causative agent of Buruli ulcer. The pathology of *M. ulcerans* disease has been attributed to the secretion of a potent macrolide cytotoxin known as mycolactone which plays an important role in the virulence of the disease. Mycolactone is a biomarker for the diagnosis of BU that can be detected using the fluorescent-thin layer chromatography (f-TLC) technique. The technique relies on the chemical derivatization of mycolactone A/B with 2-naphthylboronic acid (BA) which acts as a fluorogenic chemosensor. However, background interferences due to co-extracted human tissue lipids, especially with clinical samples coupled with the subjectivity of the method call for an investigation to find an alternative to BA.

Methods Twenty-six commercially available arylboronic acids were initially screened as alternatives to BA using the f-TLC experiment. UV-vis measurements were also conducted to determine the absorption maximum spectra of mycolactone A/B and myco-boronic acid adducts followed by an investigation of the fluorescence-enhancing ability of the boronate ester formation between mycolactone A/B and our three most promising boronic acids (BA15, BA18, and BA21). LC-MS technique was employed to confirm the adduct formation between mycolactone and boronic acids. Furthermore, a comparative study was conducted between BA18 and BA using 6 Polymerase Chain Reaction (PCR) confirmed BU patient samples.

Results Three of the boronic acids (BA15, BA18, and BA21) produced fluorescent band intensities superior to BA. Complexation studies conducted on thin layer chromatography (TLC) using 0.1 M solution of the three boronic acids and various volumes of 10 ng/μL of synthetic mycolactone ranging from 1 μL – 9 μL corresponding to 10 ng – 90 ng gave similar results with myco-BA18 adduct emerging with the most visibly intense fluorescence bands. UV-vis absorption maxima (λ_{\max}) for the free mycolactone A/B was observed at 362 nm, and the values for the adducts myco-BA15, myco-BA18, and myco-BA21 were at 272 nm, 270 nm, and 286 nm respectively. The comparable experimental λ_{\max} of 362 nm for mycolactone A/B to the calculated Woodward-Fieser value of 367 nm for the fatty acid side chain of mycolactone A/B demonstrate that even though 2 cyclic boronates were formed, only the boronate of the southern side chain with the chromophore was excited by irradiation at 365 nm. Fluorescence experiments have demonstrated that coupling BA18 to mycolactone A/B along the 1,3-diols remarkably enhanced the fluorescence intensity at 537 nm. High-Resolution Mass Spectrometer (HR-MS) was used to confirm the formation of the

*Correspondence:

Richard K. Amewu
ramewu@ug.edu.gh

Full list of author information is available at the end of the article



© The Author(s) 2023. **Open Access** This article is licensed under a Creative Commons Attribution 4.0 International License, which permits use, sharing, adaptation, distribution and reproduction in any medium or format, as long as you give appropriate credit to the original author(s) and the source, provide a link to the Creative Commons licence, and indicate if changes were made. The images or other third party material in this article are included in the article's Creative Commons licence, unless indicated otherwise in a credit line to the material. If material is not included in the article's Creative Commons licence and your intended use is not permitted by statutory regulation or exceeds the permitted use, you will need to obtain permission directly from the copyright holder. To view a copy of this licence, visit <http://creativecommons.org/licenses/by/4.0/>. The Creative Commons Public Domain Dedication waiver (<http://creativecommons.org/publicdomain/zero/1.0/>) applies to the data made available in this article, unless otherwise stated in a credit line to the data.

myco-BA15 adduct. Finally, f-TLC analysis of patient samples with BA18 gave improved BA18-adduct intensities compared to the original BA-adduct.

Conclusion Twenty-six commercially available boronic acids were investigated as alternatives to BA, used in the f-TLC analysis for the diagnosis of BU. Three (3) of them BA15, BA18, and BA21 gave superior fluorescence band intensity profiles. They gave profiles that were easier to interpret after the myco-boronic acid adduct formation and in experiments with clinical samples from patients with BA18 the best. BA18, therefore, has been identified as a potential alternative to BA and could provide a solution to the challenge of background interference of co-extracted human tissue lipids from clinical samples currently associated with the use of BA.

Keywords Buruli ulcer, Arylboronic acid, *Mycobacterium ulcerans*, Buruli ulcer, Mycolactone

Background

Mycolactone (ML), the first macrolide cytotoxin known to be produced by a human pathogen *Mycobacterium ulcerans* (MU) is the causative agent of Buruli ulcer (BU) [1, 2]. It is the only macrolide identified in the genus *Mycobacterium* [3]. In 1965, Connor and co-workers hypothesized that *M. ulcerans* was responsible for the production of the diffusible cytotoxin which was subsequently confirmed using guinea pigs. Injection of mycobacterial culture filtrates into the experimental animal resulted in necrosis like those of human infections [4–6]. The suspected molecule was later effectively isolated, purified, and characterized from the acetone-soluble portion of lipid extracts of *M. ulcerans* in 1999 by George et al. The chemical structure was subsequently solved as a polyketide named mycolactone (ML) [7, 8]. ML was detected on thin layer chromatography (TLC) as a light yellow, ultraviolet-active lipid band with a retention factor value of 0.23 in chloroform/methanol/water

(90:10:1, vol/vol/vol) [7]. A prominent peak at m/z 765, corresponding to the sodium adduct of mycolactone was observed by mass spectrometry (MS) analysis under electrospray conditions. ML is a hybrid polyketide macrolide with a 12-membered lactone ring at its core, along with a C5-O-linked polyunsaturated acyl side chain numbered C1'–C16' to the south and a C-linked upper side chain numbered C12–C20 to the north. Different congeners of mycolactone result from differences in the "Southern" chain, while the upper "Northern" chain is invariant. Further research revealed that the mycolactone obtained from *M. ulcerans* was a 3:2 combination of the two stereoisomers known as mycolactones A and B, which form as spontaneous geometric isomers around the double bond at C4' C5' (shown by the wavy line between C5' and C6') [9, 10] (Fig. 1).

The pathology of *M. ulcerans* disease has been largely attributed to the secretion of this potent cytotoxin, a substance crucial to the pathogenicity of the disease [7].

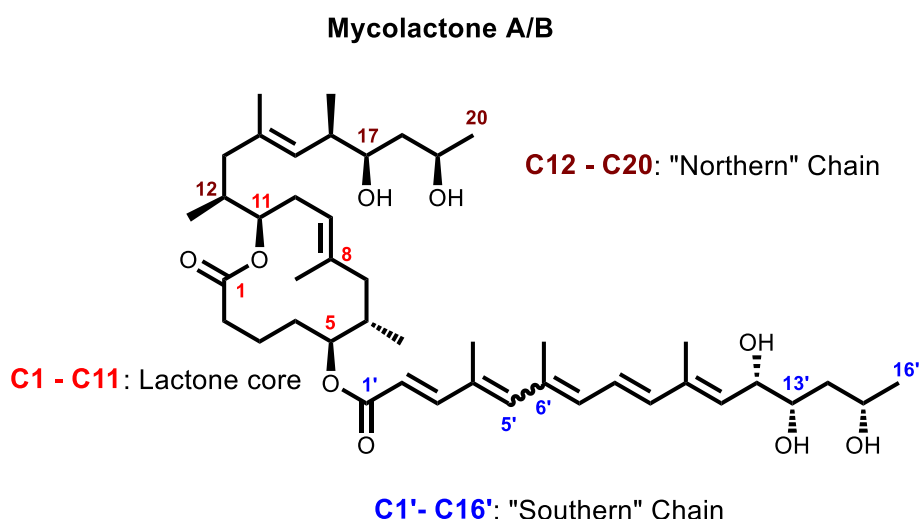


Fig. 1 Structure of mycolactone A/B. Mycolactone A/B has a core cyclic lactone ring (C1–C11) and two highly unsaturated acyl side chains produced from polyketides. The longer "Southern" chain is numbered C1'–C16', and the upper "Northern" chain is made up of C12–C20. Mycolactone exists as a 3:2 ratio of spontaneously generating geometric isomers around the double bond at C4' C5' (depicted by the wavy line between C5' and C6')

Tissue necrosis, painlessness, and immunosuppressive properties have all been attributed by various reports to the toxin [11, 12]. Mycolactone A/B diffuses outside the sites of the original infection hence it is an interesting target for detection in circulating blood cells [13].

Since the toxin is only produced by *M. ulcerans*, mycolactone is being investigated as a biomarker for the diagnosis of Buruli ulcer disease. Methods including thin-layer chromatography (TLC) [7, 8], mass spectrometry [14–16], or cytotoxicity assays [15] have been developed to detect and quantify mycolactone in tissue samples towards the diagnosis of the BU disease. Mycolactone has recently been investigated in patient biopsy samples using LC–MS [15, 17] and RNA aptamer binding [18].

For diagnosis purposes, a very sensitive, practical, and relatively economical and simple to use fluorescent-thin layer chromatography (*f*-TLC) method for the detection of the mycolactones produced by the human pathogen, *Mycobacterium ulcerans* was developed by Kishi and colleagues [19]. In the method, mycolactone A/B was chemically derivatized using 2-naphthylboronic acid (BA) as a fluorogenic chemosensor (Fig. 2). The 1,3-diol units on the side chains of mycolactone A/B complex with the boronic acid to generate two 6-membered cyclic boronate rings. When the pentaenoate chromophore on the southern side chain was irradiated at 365 nm wavelength, the enhanced fluorescence emission from the C13', C15'-cyclic boronate was observed at the chromophore emission wavelength of 520 nm [19] (Fig. 2).

Boronic acids have previously been coupled with *cis*-1,2- and 1,3-diols to generate reversible five- or six-membered cyclic boronate esters [20–23]. Fluorescence can be greatly impacted by the formation of

boronate esters. The first report on the use of boronic acid as a receptor for saccharide sensing was made in 1992 by Yoon and Czarnik [24]. Since then, numerous biomedical applications have utilised the distinct recognition properties of boronic acids and boronic acid analogues against 1,2- or 1,3-diols [25]. In the area of diagnostic medicine, sensors play crucial roles in their ability to provide quick and quantitative resolution of analytes. Whyte and co-workers showed that boronic acids are reliable sensors for a variety of saccharides, polysaccharides, glycoproteins, glycosylated proteins, and dopamine [25].

Furthermore, boronic acid sensors have been developed to measure blood glucose levels [26–30], ionic compounds [31–33], water traces in solvents [34, 35], hydrogen peroxide (H₂O₂) [36, 37], and catecholamines [38]. Boronic acids have also been employed as biochemical tools for a variety of applications, including tumor cell imaging [39, 40], enzyme inhibitors [41], and cell delivery methods [42]. For these reasons, boron-based fluorescence sensors are crucial in current research.

The detection of mycolactone by coupling to BA has been successfully demonstrated [19, 43–45]. However, concerns such as background interferences from co-extracted human tissue lipids need to be addressed. The search for a more efficient and fluorescent boronic acid as an alternative to the original BA utilized by Kishi and coworkers is required. To find possible alternatives to BA, several commercially available arylboronic acids were screened using *f*-TLC. The thin layer chromatography (TLC) of the purchased boronic acids was performed and the profile of their fluorescence band intensities was compared to BA.

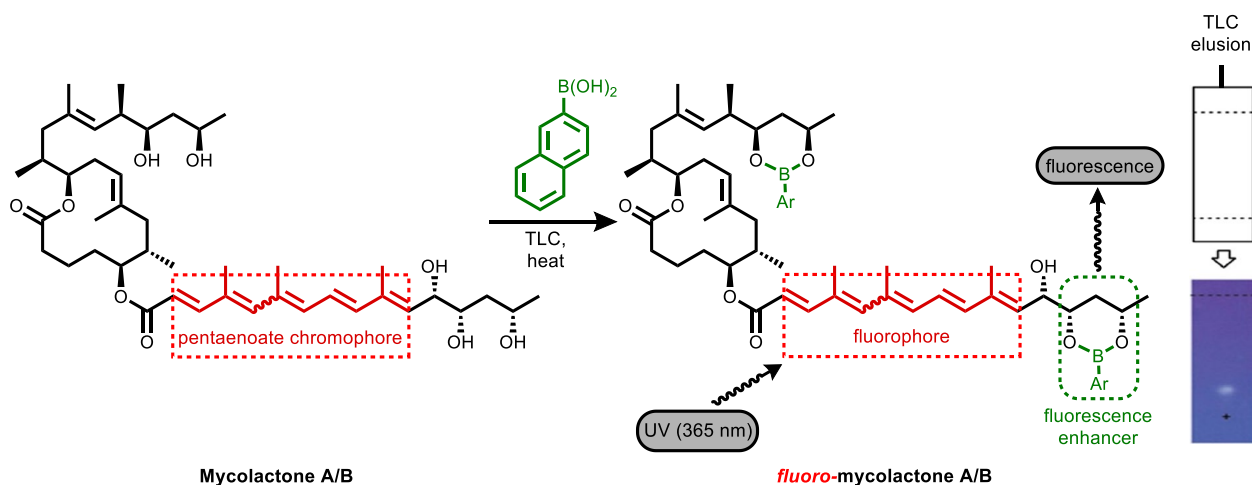


Fig. 2 Schematic illustration of fluorescent-TLC detection method showing the derivatization of mycolactone A/B with BA [19]

Materials and methods

Reagents and chemicals

Synthetic mycolactone A/B was kindly donated by Prof Kishi Yoshito (Harvard University) through the World Health Organization (WHO), Geneva, Switzerland. All twenty-six structurally diverse arylboronic acids were purchased from Sigma-Aldrich. All reagents were of analytical grade and used without further purification. Solvents are of commercial grade and were used as supplied. Fluorescent dye-free TLC silica gel 60 plates (5721–7) were purchased from EMD chemical Inc and were cut into 5×2 cm sizes for the development of the plate. The UV lamp used was a benchtop UV transilluminator (UVM-28 EL Series UV lamp 365/302 nm (8 Watt) purchased from UVP Inc.

Spotting

Solutions of 0.1 M of the various structurally diverse arylboronic acids were prepared by the addition of acetone and used according to the previous report of Kishi and co-workers [19]. Standard mycolactone A/B solution for TLC spotting was prepared from a stock solution of 0.1 mg/mL mycolactone in 0.5 mL in an ampoule. A 10 ng/μL standard solution of mycolactone A/B was prepared by taking 0.1 mL of the mycolactone stock solution into a glass vial and adding 0.9 mL ethyl acetate to give the required standard. Optimal visualization of mycolactone A/B was accomplished by spotting the standard on the silica-coated glass TLC plates, eluting with a mixture of chloroform/hexane/methanol (5:4:1; v/v/v) and finally, by slow immersion of the eluted plate in the 0.1 M boronic acid solutions, removal, and then heating the plate to a temperature of ~100 °C. The glass side of the plate was then wiped clean with an acetone-soaked tissue paper towel and then viewed by illuminating at ~365 nm using a Benchtop UV transilluminator.

Absorption spectroscopy

The absorption spectra were recorded on a Shimadzu UV-1800 Spectrophotometer. All UV–Vis absorption spectra were obtained using quartz cuvettes with a diameter of 1 cm between 200 and 800 nm.

Fluorescence spectroscopy

Fluorometric experiments were performed on both a Shimadzu Spectrofluorometer (Model RF-6000) and a Horiba Jobin Yvon (HJY) Fluoromax-3 Spectrofluorometer. Emission spectra were recorded at room temperature with excitation wavelength at 365 nm and slit widths of excitation and emission set at 5 nm and 10 nm respectively. Various dilutions of mycolactone A/B (4 to 32 μg/mL) were prepared from standard solution of mycolactone A/B (0.1 mg/mL in 0.5 mL EtOAc) as shown in the Table 1 below in 4 mL amber vials. They were diluted using cyclohexane to obtain the final concentrations.

Solutions of boronic acids 2-naphthylboronic acid (BA), [1,1':4',1''-terphenyl]-2-ylboronic acid (BA15), (9,9-Diphenyl-9H-fluoren-4-yl)boronic acid (BA18), and (3-(Naphthalen-1-yl)phenyl)boronic acid (BA21) (0.10 M) in methanol were also prepared. To perform 1 mL reactions, seven samples containing 500 μL of 0.10 M BA18 solution and 500 μL of each dilution of the mycolactone A/B (4 to 32 μg/mL) standard solution in Table 1 were dispensed into 1.5 mL microtubes and mixed well and the fluorescence spectra were recorded after 10 min (λ_{ex} 365 nm and λ_{em} from 380 to 700 nm).

General procedure for the preparation of boronate esters from corresponding diols

To a solution of diol (1 equiv.) in dichloromethane (DCM) (1 M) was added the boronic acid (1 equiv.). The resultant mixture was stirred for 30 min. The solvent was removed *in vacuo*, and the resultant residue was dried under a high vacuum (0.1 mm Hg) for 1 h. It was then

Table 1 Serial dilutions of mycolactone A/B solutions

No.	0.1 mg/mL mycolactone standard solution (μL)	Diluent (Cyclohexane) (μL)	Final concentration of mycolactone (μg/mL)	Final concentration of mycolactone (μM)
1	160	340	32	43.1
2	140	360	28	37.7
3	120	380	24	32.3
4	100	400	20	26.9
5	80	420	16	21.5
6	60	440	12	16.2
7	40	460	8	10.8
8	20	480	4	5.4
9	0	500	0 (Blank)	0

redissolved in cyclohexane and used as a stock solution for mass spectrometry analysis (Fig. 3).

LC-ESI-Q-ToF analysis

Analyses were carried out using a 1260 Infinity LC (Agilent Technologies), coupled to a Quadrupole-Time of Flight tandem mass spectrometer 6530 Infinity Q-ToF detector (Agilent Technologies) by a Jet Stream ESI interface (Agilent Technologies). The LC conditions were: Zorbax Extend-C18 column (2.1 mm × 50 mm, 1.8 μm particle size); 0.4 mL/min flow rate; 1 μL injection volume for MS experiments. and 10 μL for MSMS experiments; 40 °C column temperature. Separation was achieved using a gradient of water with 0.1% formic acid (eluent A) and acetonitrile with 0.1% formic acid (eluent B). The elution gradient was programmed as follows: initial conditions 5% B, followed by a linear gradient to 95% B in 15 min. The ESI operating conditions were drying gas (N₂, purity >98%): 350 °C and 11 L/min; capillary voltage 4.0 kV; nebulizer gas 40 psig; sheath gas (N₂, purity >98%): 375 °C and 11 L/min. High-resolution MS spectra were acquired in a positive mode in the range 100–2400 m/z.

Analysis of clinical samples using f-TLC

Clinical samples confirmed by gold standard Polymerase Chain Reaction (PCR) for IS2404 to be either BU or non-BU were analyzed by the f-TLC method using the original boronic acid BA and the most promising boronic acid, BA18 respectively. Both fine-needle aspirates (FNA) and swab samples were analyzed. Standard PCR targeting IS2404 was performed according to the protocol described by Stinear et al. [46].

Mycolactone extraction and detection by fluorescent-thin layer chromatography (f-TLC) technique was done according to the protocol published elsewhere [43]. Ethanol containing the dissolved sample was filtered through a cotton plug into a glass vial. The sample container was further rinsed with 1 mL ethyl acetate, which was added to the glass vial through a cotton plug, and the contents were evaporated to dryness under reduced pressure of about 10–15 mmHg using a rotary evaporator. To separate any contaminating solid from liquid, 100 μL hexane/ether (1:1) solution was added to the glass vial, rinsed,

and transferred by microsyringe into a clean glass vial which was air-dried. After evaporation, 50 μL hexane/ether (1:1) was added to the dry sample and 10 μL of the resuspended sample was spotted onto a 3.3 × 6.6 cm fluorescent-dye free TLC plate (TLC Silica gel 60, EMD Millipore, Darmstadt, Germany; Gibbstown, NJ, USA) alongside 50 ng synthetic mycolactone A/B standard in ethyl acetate and a co-spot of 10 μL sample with 50 ng synthetic mycolactone A/B. The plate was developed in chloroform/hexane/methanol (5:4:1; v/v/v) until the leading edge reached the top of the plate, air-dried, and dipped in 0.1 M solution of both BA and (9,9-Diphenyl-9H-fluoren-4-yl)boronic acid (BA18) in acetone, then heated for 60 s at 100 °C on a hot plate. The glass side of the plate was wiped with acetone on a paper towel. The plate was placed on a UV lamp with a 365 nm filter. The fluorescent band at a retention factor of 0.23 from the patient sample was compared to that of the standards to confirm the presence of mycolactone. The f-TLC plates were independently read by two laboratory analysts before reporting the results. The laboratory analysts who worked on both the f-TLC and PCR specimens were blinded to certain relevant clinical information (except for age, and gender) as well as diagnostic test results of each other. This was to ensure that there was no diagnosis bias [43].

Results

Fluorescent thin-layer chromatography (f-TLC) analysis

The TLC profiles of twenty-six commercially available aryl boronic acids (Additional document 1, Table S1) were obtained and their fluorescence band intensities profiles were compared to BA. A visual comparison of fluorescent bands on all the TLC profiles indicates that three of the boronic acids (BA15, BA18, and BA21) were visually superior to BA. They gave excellent and highly intense yellow fluorescence bands on a blue background of the TLC plate under 365 nm UV light than BA (Table 2). Following these promising results, the three were selected for further quantitation and spectroscopic studies.

From the prepared working concentration of 10 ng/μL of synthetic mycolactone, various volumes ranging from 1 μL – 9 μL which correspond to 10 ng – 90 ng were

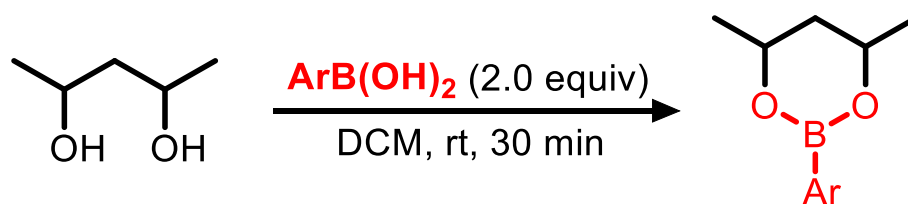
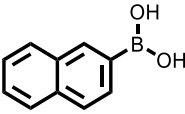

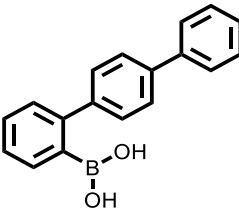

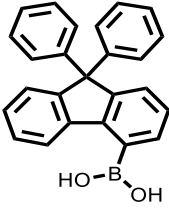

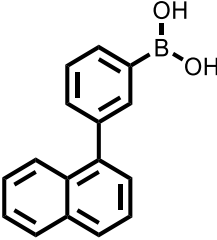



Fig. 3 Reaction of 1,3-diol with arylboronic acid to form a 6-membered cyclic boronate ester

Table 2 Structures of the original BA and 3 promising boronic acids with their corresponding TLCs

Entry	Boronic acid	Structure	TLC
BA	2-naphthylboronic acid		
BA15	[1,1':4,1''-terphenyl]-2-ylboronic acid		
BA18	(9,9-Diphenyl-9H-fluoren-4-yl)boronic acid		
BA21	(3-(Naphthalen-1-yl)phenyl)boronic acid		

spotted on the TLC plate using 1–5 μL calibrated micropipettes (Drummond Scientific). Like the observation above, the three boronic acids gave more intense fluorescent bands compared with BA for all the concentrations. Of the three new ones, BA18 produced the most visibly intense fluorescence bands (Fig. 4).

UV-vis spectra

Next, we performed UV-vis measurements to determine the absorption maximum spectra of mycolactone A/B and myco-boronic acid adducts. The UV-vis spectra of the free mycolactone A/B and its boronic acids adducts are shown in Fig. 5. The absorption maxima (λ_{max}) of the free mycolactone A/B was 362 nm while values of 272 nm, 270 nm, and 286 nm respectively were obtained for myco-BA15, myco-BA18, and myco-BA21.

Fluorescence spectra of mycolactone A/B– boronic acid complexes

In another experiment, we assessed the fluorescence-enhancing ability of the boronate ester formation between mycolactone A/B and our three most promising boronic acids (BA15, BA18, and BA21) (Fig. 6A). When mycolactone A/B was excited at 365 nm in cyclohexane, the pentaenoate gave fluorescence emission at 537 nm. After coupling BA18 to the 1,3-diol, the fluorescence intensity was remarkably enhanced at the same wavelength (Fig. 6B). The fluorescence intensity was also observed to have increased as the concentration of mycolactone increased from 0 to 20 $\mu\text{g}/\text{mL}$ Fig. 6C. When the fluorescence intensity at 537 nm was plotted against the concentration of mycolactone, a linear calibration curve with a regression coefficient of 0.93 was obtained (Fig. 6D).

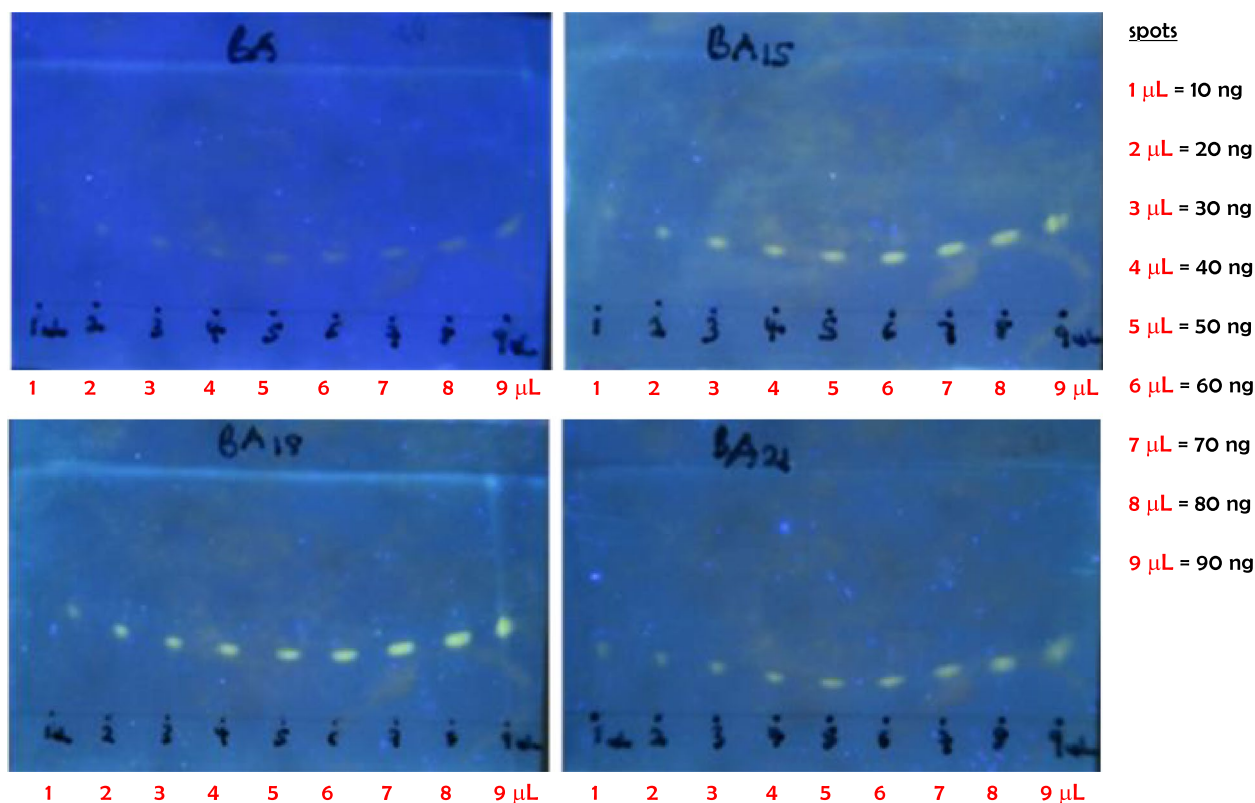


Fig. 4 Representative TLC profiles after triplicates experiments for each boronic acid (BA, BA15, BA18 and BA21). Comparison of the original boronic acid (BA) with the three most promising boronic acids (BA15, BA18, and BA21) for the detection of synthetic mycolactone A/B. Various volumes (1 – 9 μ L) of the working solution of mycolactone A/B (10 ng/mL) were spotted on a silica gel thin layer chromatography plate, dipped in 0.1 M solution of boronic acids (BA, BA15, BA18, and BA21), eluted with chloroform/hexane/methanol (5:4:1; v/v/v), heated at 100 $^{\circ}$ C, and illuminated at 365 nm with a benchtop UV transilluminator (UVLAM-28 EL Series UV lamp 365/302 nm (8 Watt)

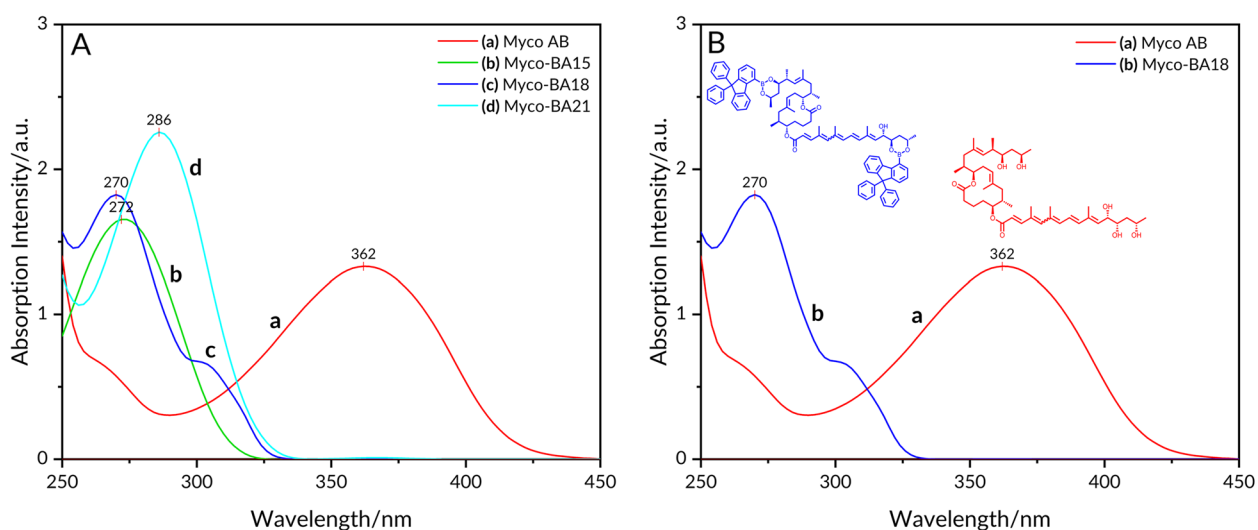


Fig. 5 Absorption spectra of mycolactone A/B and myco-boronic acid complexes. **A** (a) mycolactone A/B in MeOH (λ_{max} 362 nm); (b) mycolactone A/B – BA15 boronate complex in MeOH (λ_{max} 272 nm); (c) mycolactone A/B – BA18 boronate complex in MeOH (λ_{max} 270 nm); (d) mycolactone A/B – BA21 boronate complex in MeOH (λ_{max} 286 nm). **B** Absorption spectra (a) mycolactone A/B in MeOH (λ_{max} 362 nm); (b) mycolactone A/B – BA18 boronate complex in MeOH (λ_{max} 270 nm)

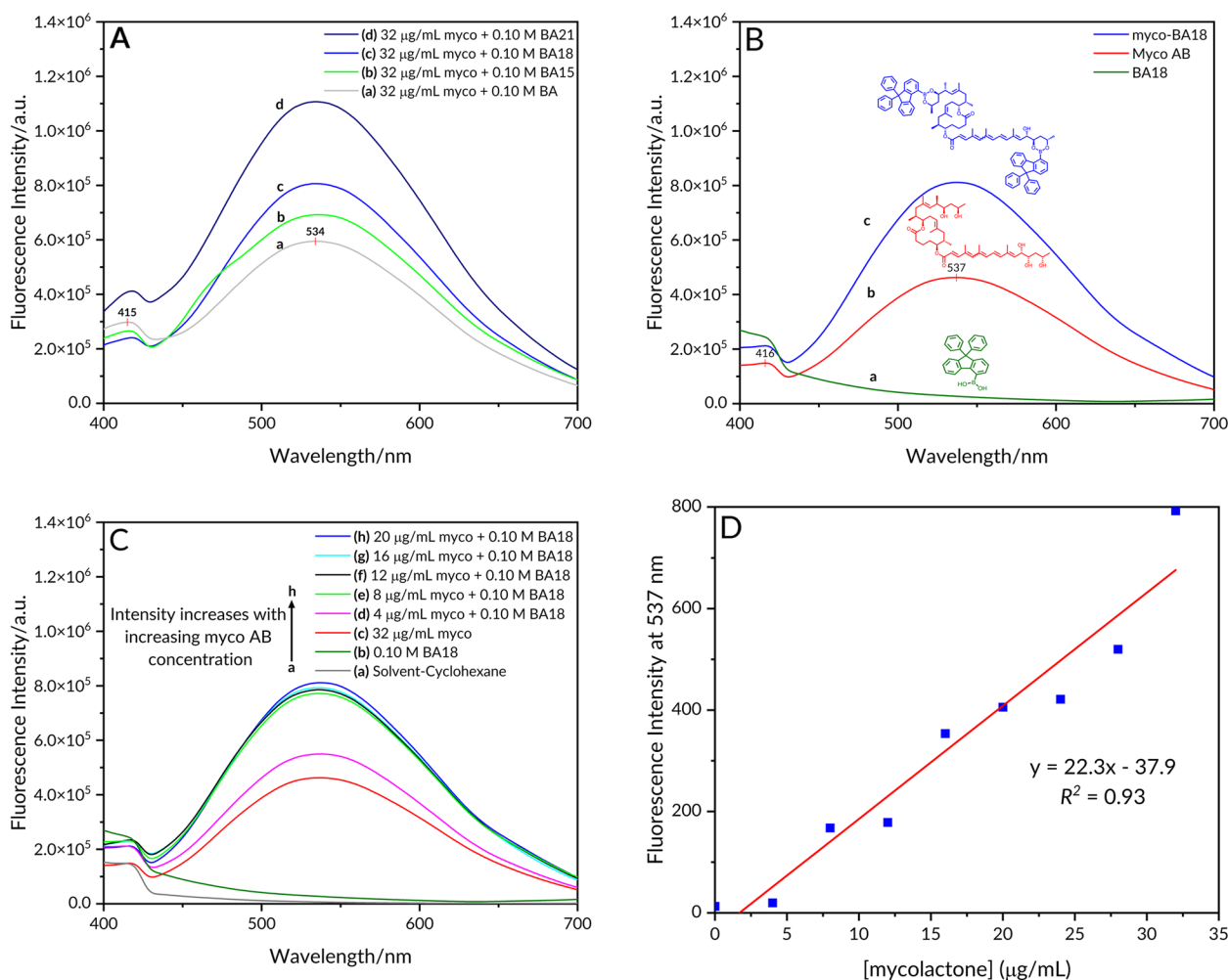


Fig. 6 Fluorescence emission spectra in cyclohexane recorded at room temperature with Horiba Jobin Yvon (HJY) Fluoromax-3 spectrofluorimeter. Excitation wavelength 365 nm (excitation slit width 5 nm, emission slit width 10 nm). **A** (a) mycolactone A/B–BA boronate complex; (b) mycolactone A/B–BA15 boronate complex; (c) mycolactone A/B–BA18 boronate complex; (d) mycolactone A/B–BA21 boronate complex; (λ_{\max} 534 nm); **B** Fluorescence emission spectra (a) BA18; (b) mycolactone A/B in cyclohexane (λ_{\max} 537 nm); (c) mycolactone A/B–BA18 boronate complex (λ_{\max} 270 nm); **C** (a) solvent (cyclohexane); (b) free BA18 (0.10 mol dm⁻³); (c) Free mycolactone (32 µg/mL); (d–h) Mycolactone A/B–boronic acid 18 complexes, BA18 concentration was fixed at 0.10 mol dm⁻³ in the mixtures, while mycolactone concentrations were 4 µg/mL, 8 µg/mL, 12 µg/mL, 16 µg/mL, and 20 µg/mL, respectively, in the mixtures; **D** A plot of fluorescence intensity at 537 nm against various concentrations of mycolactone A/B

To examine the correlation between excitation and emission spectral shifts, we plot the excitation peak versus the corresponding emission peak for myco-BA18 boronate complex in cyclohexane and methanol respectively (Fig. 7A). From the plot, we observed an emission peak maximum at a higher wavelength ($\lambda_{\text{em,max}}$ 537 nm) as compared to the excitation peak maximum ($\lambda_{\text{em,max}}$ 362 nm). We then determined the Stokes' shift for the myco-BA18 boronate complex from the excitation and emission spectral peak maxima to be 175 nm. A significant fluorescence enhancement was visually observed on the TLC at 537 nm with (blue) the boronic

acid compared to that without (red) using a 365 nm UV lamp (Fig. 7B).

Mass spectra of mycolactone–boronic acid adducts

High-resolution mass spectroscopic (MS) analysis was performed to confirm the formation of the mycolactone–BA15 adduct. First, MS analysis of mycolactone A/B was performed, and the chromatogram obtained is shown in (Figure S1). The molecular ion peak was obtained at m/z 765.4760 with a formula of C₄₄H₇₀O₉Na which corresponds to the sodium adduct of mycolactone A/B. This is consistent with previously published literature mass for

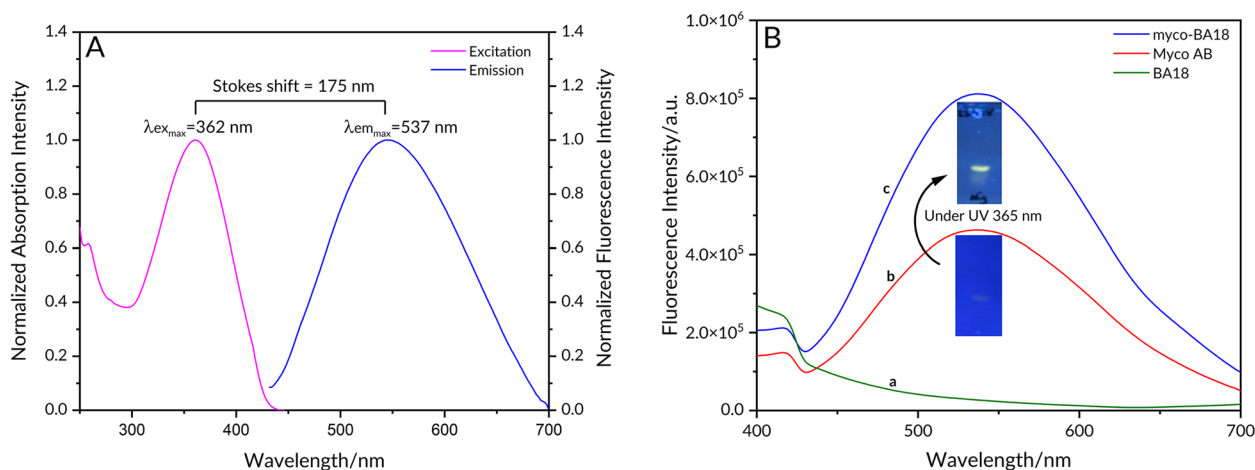


Fig. 7 **A** Emission (λ_{max} 537 nm) and its corresponding excitation (λ_{max} 362 nm) spectra obtained for myco-BA18 boronate complex in cyclohexane and methanol respectively; **B** myco-BA18 boronate complex under 365 nm UV

the toxin [7]. Then, a chemical reaction according to Fig. 8 was conducted between mycolactone A/B and the B15 after which the mass spectrometer analysis was repeated.

The success of the reaction was confirmed by HR-MS analysis. The results showed that the myco-BA15 boronate ester adduct was formed as shown in Fig. 9 below and Additional document 1, Figure S2 A new m/z signal observed at 1241.6823 corresponding to $[M+Na]^+$ is attributed to the myco-BA15 sodium adduct with elemental formula $C_{80}H_{92}B_2O_9Na$, confirming the formation of the required adduct. In addition, the MS data strongly corroborated the intensity changes observed in UV-vis and fluorescent experiments.

Validation on real samples

A comparative study between the promising boronic acid (BA18) and the original boronic acid (BA) using the f-TLC method was conducted on five (5) different PCR

positive confirmed BU patients. Two sets of measurements were conducted (Fig. 10), first, the original BA (top panel) was used to form the adducts according to previously described protocols followed by B18 (bottom panel). Like the results obtained with non-clinical samples, B18 showed an improved intensity of the myco-B18 adduct spot versus that with BA. In addition, it was easier to interpret the TLC profiles of the samples with background interference exemplified by unique identifiers SA and LN respectively. Also, four (4) different PCR negative control non-BU samples were analyzed using our most promising BA18 boronic acid to allow for comparison with the positive cases (Fig. 11). Here, it is worthy of note that despite the background interferences resulting from the co-extracted human tissue lipids from the samples, the TLC profiles clearly indicated negative results because the BA18 is strongly fluorescent as compared to the original BA as presented on the top panel of Fig. 10.

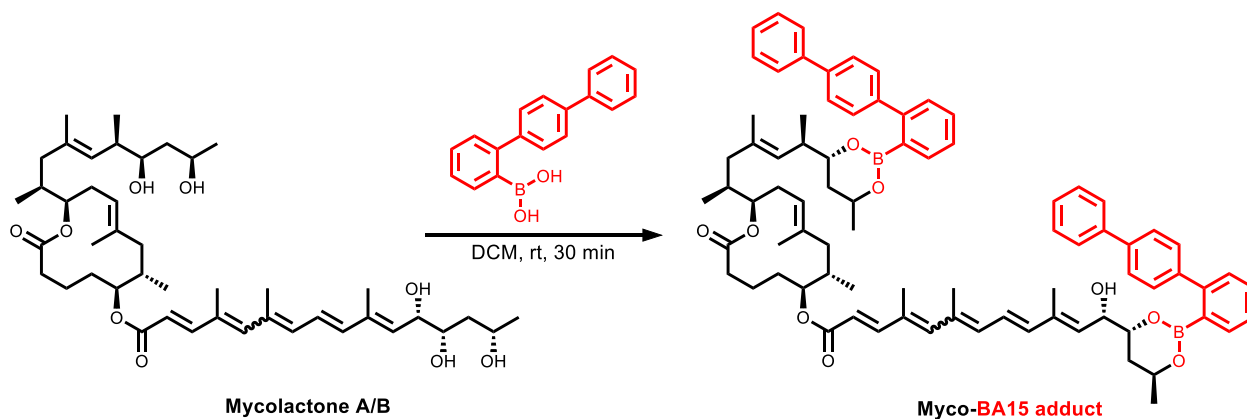


Fig. 8 Proposed complexation reaction between boronate 1,3-diols of mycolactone A/B and BA15 to form cyclic boronate adduct

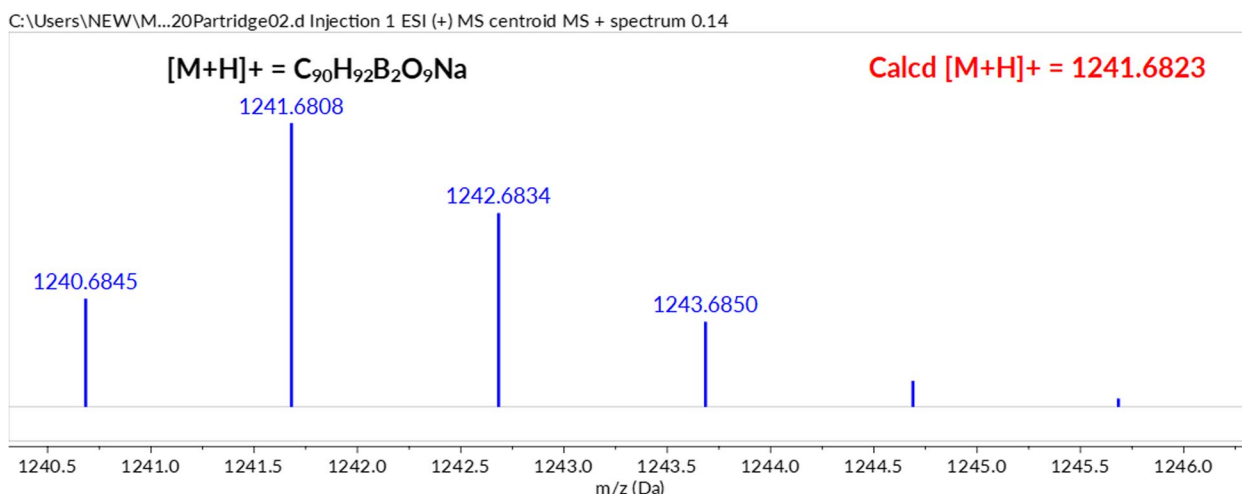


Fig. 9 Electrospray ionization (ESI) mass spectrum of mycolactone A/B-BA15 boronate adduct

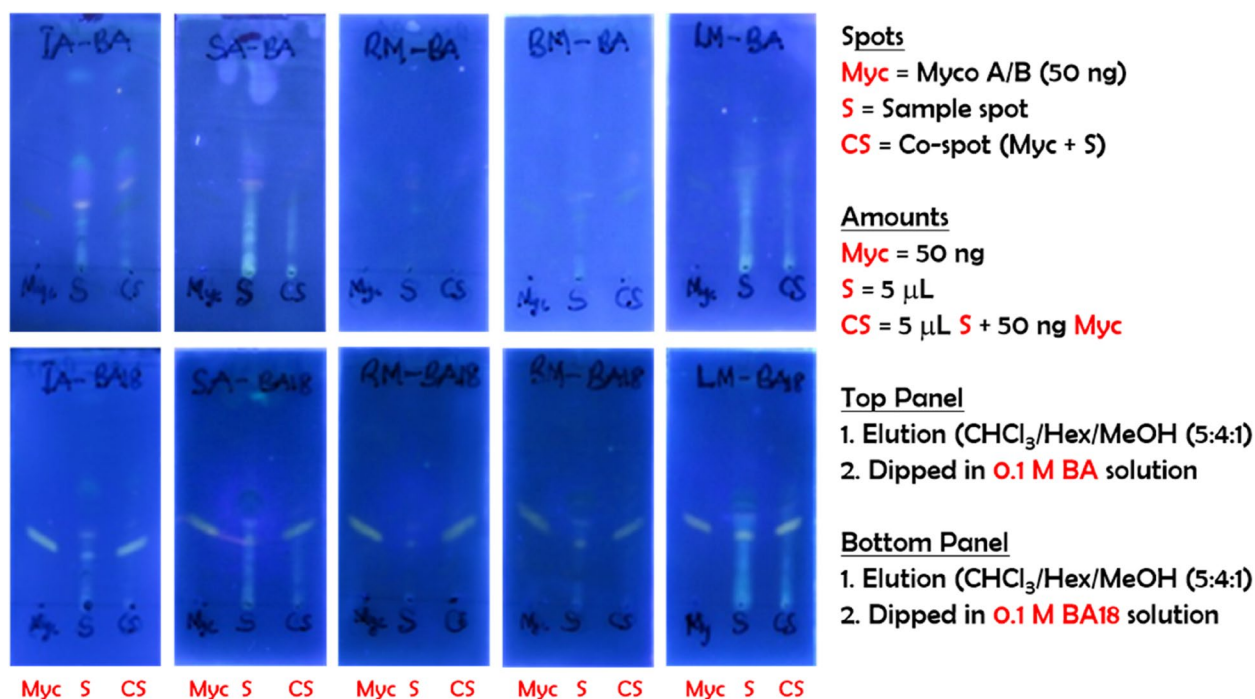


Fig. 10 f-TLC plates of clinical samples from 5 different PCR positive confirmed BU cases. Each TLC plate is marked with three spots, Myco, S and CS for synthetic mycolactone A/B, sample and co-spot respectively. The samples were applied at the same concentration and the plates were developed using chloroform/hexane/methanol (5:4:1; v/v/v)

Discussion

Prior to direct observation under a 365 nm UV light, fluorescent complexation reactions of various commercially available arylboronic acids with the 1,3-diol moieties on the mycolactone A/B structure on a TLC surface were carried out. Mycolactone A/B is weakly fluorescent in its free form; however, it becomes fluorescent when bound

to an appropriate boronic acid. BA has been the boronic acid of choice for the f-TLC method [19].

Woodward-Fieser rule has been employed in correlating electronic transitions and structures of α,β-unsaturated ketones as well as forecasting the position of the longest wavelength π → π* band of these compounds [47, 48]. Here, we used the Woodward-Fieser

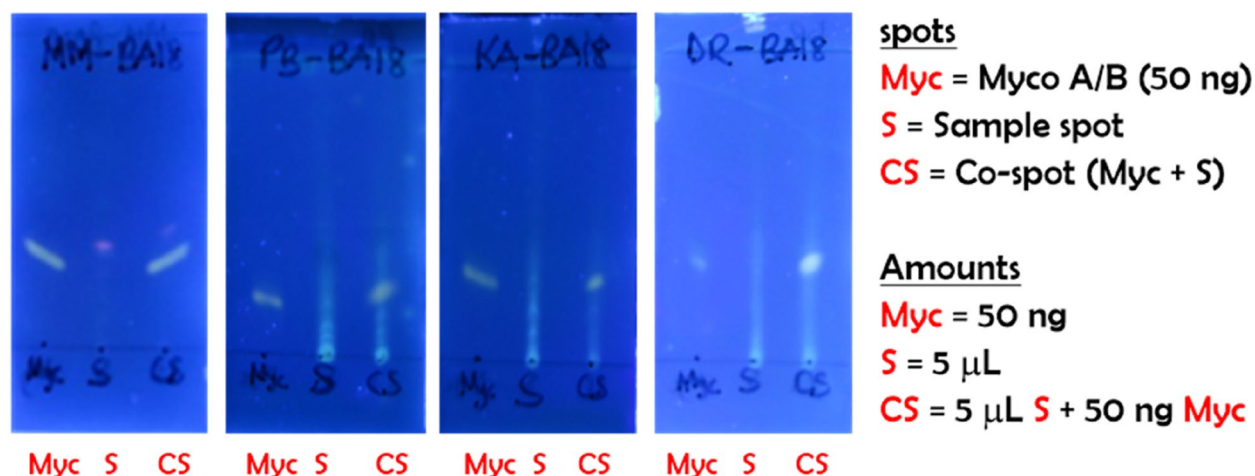


Fig. 11 f-TLC plates of clinical samples from 4 different PCR negative confirmed non-BU cases. Each TLC plate is marked with three spots, Myco, S and CS for synthetic mycolactone A/B, sample, and co-spot respectively. The samples were applied at the same concentration and the plates were developed using chloroform/hexane/methanol (5:4:1; v/v/v)

rule to calculate a predicted empirical wavelength for the lowest energy $\pi \rightarrow \pi^*$ electronic transition of mycolactone. For α,β -unsaturated esters, the base value is 215 nm. A total of 4 additional double bonds from the pentaenoate region (+30 each), and 3 methyl-substituted double bonds contributing +18 each were added. The sum of the calculated absorption maximum was 367 nm compared to the experimental value of 362 nm as measured on UV. This is consistent with the UV-vis analysis of the fatty acid side chain of mycolactone A/B [44]. These findings demonstrate that even though 2 cyclic boronates are formed, one on the southern side chain diol and the other on the northern side chain, only the boronate of the southern side chain with the chromophore was excited by irradiation through a 365 nm filter. The boronate on the upper chain, however, was not excited and hence did not contribute to the enhanced fluorescence under UV light [49]. The arylboronate formed has the potential to enhance fluorescence emission [44, 45]. This is because the excitation of mycolactone alone presented weak fluorescence at 537 nm with a Stokes shift of 175 nm (Fig. 7A). However, after the complexation was triggered with the boronic acid, a significant turn-on fluorescent enhancement was observed at the same 537 nm, and the fluorescence was also visually observed on TLC using a UV lamp, as shown in Fig. 7B. Thus, the change in fluorescence intensity of mycolactone A/B is attributed to an energy transfer from the excited pentaenoate motif which serves as a fluorophore to a fluorogenic acceptor in the form of the arylboronic acid (BA18) [19].

Conclusions

Twenty-six commercially available arylboronic acids were screened as potential alternatives for BA. TLC analyses of the purchased boronic acids were performed and their fluorescence band intensities profiles were compared to the original BA. The boronic acids readily form arylboronate ester complexes with mycolactone A/B and three of them gave superior fluorescence band intensities. A repeat of the complexation of the boronic acids BA, BA15, BA18, and BA21 in serially diluted BA from 10 ng/ μ L – 90 ng/ μ L gave similar results with BA18 emerging as the most visibly intense fluorescence bands.

When UV-vis measurements were performed with mycolactone A/B and myco-boronic acid adducts. Absorption maxima (λ_{max}) of 362 nm for mycolactone A/B was obtained while that of BA15, BA18, and BA21 were 272 nm, 270 nm, and 286 nm respectively. Applying the Woodward-Fieser rule, only the boronate of the southern side chain with the chromophore was excited by irradiation through a 365 nm filter while that of the northern side was not.

The fluorescence intensity of the boronate ester formation between mycolactone A/B and boronic acids increased as the concentration of mycolactone increased and the formation of the myco-BA15 boronate ester adduct was confirmed by HR-MS. Finally, a comparative study between BA18 and BA using PCR confirmed patient samples gave an improved intensity of the adduct and an easier to interpret TLC profiles of the samples even for those with background interference.

Abbreviations

f-TLC	Fluorescent-thin layer chromatography
TLC	Thin layer chromatography
BU	Buruli ulcer
Non-BU	Non-Buruli ulcer
HR-MS	High Resolution Mass Spectrometry
MU	<i>Mycobacterium ulcerans</i>
PCR	Polymerase Chain Reaction
UV	Ultraviolet
LAMP	Loop-mediated isothermal amplification
RNA	Ribonucleic acid
WHO	World Health Organization
Q-ToF	Quadrupole-Time of Flight tandem mass spectrometer

Supplementary Information

The online version contains supplementary material available at <https://doi.org/10.1186/s12879-023-08426-2>.

Additional file 1: Table S1. List of attempted boronic acids with their corresponding TLCs. **Figure S1.** ESI mass spectrum of mycolactone A/B. **Figure S2.** ESI mass spectrum of mycolactone A/B–BA15 boronate adduct.

Acknowledgements

We would like to acknowledge the Global Challenge Research fund (GCRF) (RBV1, UG) for supporting the work. The authors are grateful to Professor Kishi Yoshito for generously donating synthetic mycolactone A/B through the World Health Organization for the study. The authors are also grateful to Kabiru Mohammed Abass and his entire team at Agogo Presbyterian Hospital, Ghana where the patient samples came from. Above all, we are indebted to all the patients.

Authors' contributions

GAA, BMP, TDC and RKA conceptualized the project idea. GAA, BMP, TDC and RKA designed the project and GAA predominantly undertook laboratory work, analyzed and interpreted the data and prepared the original draft manuscript. All authors made important contributions and have read and approved the final version of the manuscript.

Funding

Funding for the study was provided by the Global Challenge Research fund (GCRF) (164187, University of Sheffield, RBV1, UG).

Availability of data and materials

All data generated or analyzed during this study are included in this published article and its supplementary information files.

Declarations

Ethics approval and consent to participate

This study was carried out at the Department of Chemistry, University of Ghana. Clinical samples were taken at Agogo Presbyterian Hospital, Ghana as part of the routine diagnostic procedure and case confirmation recommended by the World Health Organization (WHO) and sent to the DC for f-TLC analysis. The study was conducted according to the guidelines of the Declaration of Helsinki and approved by the Institutional Review Board of Noguchi Memorial Institute of Medical Research (NMIMR) (Study number: NMIMR-IRB CPN 024/18–19). In addition, written consent was obtained from all adult participants and legal guardians, or parents of any child participant provided informed written consent on the child's behalf. To ensure anonymity, personal information such as names, and other personal identifiers associated with patient's samples were replaced with codes.

Consent for publication

Not applicable.

Competing interests

The authors declare no competing interests.

Author details

¹Department of Chemistry, School of Physical and Mathematical Sciences, College of Basic and Applied Sciences, University of Ghana, P.O. Box LG 56, Legon, Accra, Ghana. ²Department of Chemistry, University of Sheffield, Dainton Building, Sheffield S3 7HF, UK.

Received: 28 December 2022 Accepted: 25 June 2023

Published online: 27 July 2023

References

- Doig KD, Holt KE, Fyfe JA. On the origin of *Mycobacterium ulcerans*, the causative agent of Buruli ulcer. *BMC Genomics*. 2012;13:258–77.
- George KM, Pascopella L, Welty DM. A *Mycobacterium ulcerans* toxin, mycolactone, causes apoptosis in guinea pig ulcers and tissue culture cells. *Infect Immunol*. 2000;68:877–83.
- Gunawardana G, Chatterjee D, George KM, Brennan P, Whittren D, Small PLC. Characterization of Novel Macrolide Toxins, Mycolactones A and B, from a Human Pathogen, *Mycobacterium ulcerans*. *J Am Chem Soc*. 1999;121(25):6092–3.
- Connor DH, Lunn HF. *Mycobacterium ulcerans* infection (with comments on pathogenesis). *Int J Lepr*. 1965;33(3):Suppl:698-709.
- Krieg RE, Hockmeyer WT, Connor DH. Toxin of *Mycobacterium ulcerans*. Production and effects in guinea pig skin. *Arch Dermatol*. 1974;110(5):783–8.
- Read JK, Heggie CM, Meyers WM, Connor DH. Cytotoxic activity of *Mycobacterium ulcerans*. *Infect Immun*. 1974;9(6):1114–22.
- George KM, Chatterjee D, Gunawardana G, Welty D, Hayman J, Lee R, et al. Mycolactone: a polyketide toxin from *Mycobacterium ulcerans* required for virulence. *Science*. 1999;283(5403):854–7.
- George KM, Pascopella L, Welty DM, Small PL. A *Mycobacterium ulcerans* toxin, mycolactone, causes apoptosis in guinea pig ulcers and tissue culture cells. *Infect Immun*. 2000;68(2):877–83.
- Benowitz AB, Fidanze S, Small PL, Kishi Y. Stereochemistry of the core structure of the mycolactones. *J Am Chem Soc*. 2001;123(21):5128–9.
- Fidanze S, Song F, Szlosek-Pinaud M, Small PL, Kishi Y. Complete structure of the mycolactones. *J Am Chem Soc*. 2001;123(41):10117–8.
- Hong H, Demangel C, Pidot SJ, Leadlay PF, Stinear T. Mycolactones: immunosuppressive and cytotoxic polyketides produced by aquatic mycobacteria. *Nat Prod Rep*. 2008;25(3):447–54.
- Marion E, Song OR, Christophe T, Babonneau J, Fenistein D, Eyer J, et al. Mycobacterial toxin induces analgesia in buruli ulcer by targeting the angiotensin pathways. *Cell*. 2014;157(7):1565–76.
- Hong H, Coutanceau E, Leclerc M, Caleechurn L, Leadlay PF, Demangel C. Mycolactone diffuses from *Mycobacterium ulcerans*-infected tissues and targets mononuclear cells in peripheral blood and lymphoid organs. *PLoS Negl Trop Dis*. 2008;2(10):e325.
- Sarfo FS, Phillips RO, Rangers B, Mahrous EA, Lee RE, Tarelli E, et al. Detection of Mycolactone A/B in *Mycobacterium ulcerans*-Infected Human Tissue. *PLoS Negl Trop Dis*. 2010;4(1):e577.
- Sarfo FS, Phillips RO, Zhang J, Abass MK, Abotsi J, Amoako YA, et al. Kinetics of mycolactone in human subcutaneous tissue during antibiotic therapy for *Mycobacterium ulcerans* disease. *BMC Infect Dis*. 2014;14:202.
- Sarfo FS, Converse PJ, Almeida DV, Zhang J, Robinson C, Wansbrough-Jones M, et al. Microbiological, histological, immunological, and toxin response to antibiotic treatment in the mouse model of *Mycobacterium ulcerans* disease. *PLoS Negl Trop Dis*. 2013;7(3):e2101.
- Hong H, Gates PJ, Staunton J, Stinear T, Cole ST, Leadlay PF, et al. Identification using LC-MSn of co-metabolites in the biosynthesis of the polyketide toxin mycolactone by a clinical isolate of *Mycobacterium ulcerans*. *Chem Commun (Camb)*. 2003;22:2822–3.
- Sakya SA, Aboagye SY, Otchere ID, Liao AM, Caltagirone TG, Yeboah-Manu D. RNA Aptamer That Specifically Binds to Mycolactone and Serves as a Diagnostic Tool for Diagnosis of Buruli Ulcer. *PLoS Negl Trop Dis*. 2016;10(10):e0004950.
- Spangenberg T, Kishi Y. Highly sensitive, operationally simple, cost/time effective detection of the mycolactones from the human pathogen *Mycobacterium ulcerans*. *Chem Commun (Camb)*. 2010;46(9):1410–2.

20. Tharmaraj V, Pitchumani K. d-Glucose sensing by (E)-4-((pyren-1-ylmethyl)amino)phenyl) boronic acid via a photoinduced electron transfer (PET) mechanism. *RSC Adv.* 2013;3(29):11566–70.
21. Curtius H, Kaiser G, Müller E, Bosbach D. Radionuclide release from research reactor spent fuel. *J Nucl Mater.* 2011;416(1):211–5.
22. Wu X, Chen X-X, Jiang Y-B. Recent advances in boronic acid-based optical chemosensors. *Analyst.* 2017;142(9):1403–14.
23. Hall DG. *Boronic Acids.* 2011.
24. Yoon J, Czarnik AW. Fluorescent chemosensors of carbohydrates. A means of chemically communicating the binding of polyols in water based on chelation-enhanced quenching. *J Am Chem Soc.* 1992;114(14):5874–5.
25. Whyte GF, Vilar R, Woscholski R. Molecular recognition with boronic acids-applications in chemical biology. *J Chem Biol.* 2013;6(4):161–74.
26. Kaur G, Fang H, Gao X, Li H, Wang B. Substituent effect on anthracene-based bisboronic acid glucose sensors. *Tetrahedron.* 2006;62(11):2583–9.
27. Wu W, Mitra N, Yan EC, Zhou S. Multifunctional hybrid nanogel for integration of optical glucose sensing and self-regulated insulin release at physiological pH. *ACS Nano.* 2010;4(8):4831–9.
28. Wu W, Zhou T, Berliner A, Banerjee P, Zhou S. Glucose-Mediated Assembly of Phenylboronic Acid Modified CdTe/ZnTe/ZnS Quantum Dots for Intracellular Glucose Probing. *Angew Chem Int Ed.* 2010;49(37):6554–8.
29. Huang Y-J, Ouyang W-J, Wu X, Li Z, Fossey JS, James TD, et al. Glucose sensing via aggregation and the use of “knock-out” binding to improve selectivity. *J Am Chem Soc.* 2013;135(5):1700–3.
30. Zhai W, Male L, Fossey JS. Glucose selective bis-boronic acid click-fluor. *Chem Commun.* 2017;53(14):2218–21.
31. Zhu X, Zhou X, Xing D. Ultrasensitive and selective detection of mercury (II) in aqueous solution by polymerase assisted fluorescence amplification. *Biosens Bioelectron.* 2011;26(5):2666–9.
32. Guan R, Chen H, Cao F, Cao D, Deng Y. Two fluorescence turn-on chemosensors for cyanide anions based on pyridine cation and the boronic acid moiety. *Inorg Chem Commun.* 2013;38:112–4.
33. Lee SA, You GR, Choi YW, Jo HY, Kim AR, Noh I, et al. A new multifunctional Schiff base as a fluorescence sensor for Al³⁺ and a colorimetric sensor for CN⁻ in aqueous media: an application to bioimaging. *Dalton Trans.* 2014;43(18):6650–9.
34. Ooyama Y, Furue K, Uenaka K, Ohshita J. Development of highly-sensitive fluorescence PET (photo-induced electron transfer) sensor for water: anthracene–boronic acid ester. *RSC Adv.* 2014;4(48):25330–3.
35. Ooyama Y, Matsugasako A, Oka K, Nagano T, Sumomogi M, Komaguchi K, et al. Fluorescence PET (photo-induced electron transfer) sensors for water based on anthracene–boronic acid ester. *Chem Commun.* 2011;47(15):4448–50.
36. Chung C, Srikun D, Lim CS, Chang CJ, Cho BR. A two-photon fluorescent probe for ratiometric imaging of hydrogen peroxide in live tissue. *Chem Commun.* 2011;47(34):9618–20.
37. Nonaka H, An Q, Sugihara F, Doura T, Tsuchiya A, Yoshioka Y, et al. Phenylboronic Acid-based 19F MRI Probe for the Detection and Imaging of Hydrogen Peroxide Utilizing Its Large Chemical-Shift Change. *Anal Sci.* 2015;31(4):331–5.
38. Chaicham A, Sahasithiwat S, Tuntulani T, Tomapatanaget B. Highly effective discrimination of catecholamine derivatives via FRET-on/off processes induced by the intermolecular assembly with two fluorescence sensors. *Chem Commun.* 2013;49(81):9287–9.
39. Chang M-H, Chang C-N. Synthesis of three fluorescent boronic acid sensors for tumor marker Sialyl Lewis X in cancer diagnosis. *Tetrahedron Lett.* 2014;55(32):4437–41.
40. Chu Y, Wang D, Wang K, Liu ZL, Weston B, Wang B. Fluorescent conjugate of sLex-selective bisboronic acid for imaging application. *Bioorg Med Chem Lett.* 2013;23(23):6307–9.
41. Fu H, Fang H, Sun J, Wang H, Liu A, Sun J, et al. Boronic acid-based enzyme inhibitors: a review of recent progress. *Curr Med Chem.* 2014;21(28):3271–80.
42. Cai B, Luo Y, Guo Q, Zhang X, Wu Z. A glucose-sensitive block glycopolymer hydrogel based on dynamic boronic ester bonds for insulin delivery. *Carbohydr Res.* 2017;445:32–9.
43. Amewu RK, Akolgo GA, Asare ME, Abdulai Z, Ablordey AS, Asiedu K. Evaluation of the fluorescent-thin layer chromatography (f-TLC) for the diagnosis of Buruli ulcer disease in Ghana. *PLoS ONE.* 2022;17(8):e0270235.
44. Amewu RK, Spangenberg T. Detection of Mycolactone Mycolactones by Thin Layer Chromatography Thin layer chromatography (TLC). In: Pluschke G, Röltgen K, editors. *Mycobacterium ulcerans: Methods and Protocols.* Springer, US: New York; 2022. p. 131–49.
45. Wadagni A, Frimpong M, Phanzu DM. Simple, rapid Mycobacterium ulcerans disease diagnosis from clinical samples by fluorescence of mycolactone on thin layer chromatography. *PLoS Negl Trop Dis.* 2015;9:e0004247–55.
46. Stinear T, Ross BC, Davies JK, Marino L, Robins-Browne RM, Oppedisano F, et al. Identification and characterization of IS 2404 and IS 2606: two distinct repeated sequences for detection of Mycobacterium ulcerans by PCR. *J Clin Microbiol.* 1999;37(4):1018–23.
47. Liljefors T, Allinger NL. Conformational analysis. 128. The Woodward-Fieser rules and α , β -unsaturated ketones. *J Am Chem Soc.* 1978;100(4):1068–73.
48. Tan B, Soderstrom DN. Qualitative aspects of UV-vis spectrophotometry of beta-carotene and lycopene. *J Chem Educ.* 1989;66(3):258.
49. Yable DK, Canale L, Dupuis P, Haba TC, Zoueu JT, Zissis G, editors. *Characterization and Optical Early Diagnosis by Diffuse Reflectance Spectroscopy. 2020 IEEE International Conference on Environment and Electrical Engineering and 2020 IEEE Industrial and Commercial Power Systems Europe (EEEIC / I&CPS Europe); 2020.*

Publisher's Note

Springer Nature remains neutral with regard to jurisdictional claims in published maps and institutional affiliations.

Ready to submit your research? Choose BMC and benefit from:

- fast, convenient online submission
- thorough peer review by experienced researchers in your field
- rapid publication on acceptance
- support for research data, including large and complex data types
- gold Open Access which fosters wider collaboration and increased citations
- maximum visibility for your research: over 100M website views per year

At BMC, research is always in progress.

Learn more biomedcentral.com/submissions

